


Essay

Research on the Propagation Law of Fire Smoke on the Working Face of a Belt Conveyor

Yinshang Wei, Anquan Li ^{*}, Yi Li and Wei Liang

Collage of Safety Science and Engineering, Xi'an University of Science and Technology, Xi'an 710054, China; weiys@xust.edu.cn (Y.W.); 22220226063@stu.xust.edu.cn (Y.L.); 23220089014@stu.xust.edu.cn (W.L.)

* Correspondence: 22220089031@stu.xust.edu.cn

Abstract: In view of the spread and distribution of high-temperature toxic smoke on the working face during belt conveyor fires, the FDS was used to carry out numerical simulation, establish a belt conveyor fire simulation model, set up a variety of working conditions, and study the flue gas spread of the working face with different ignition source locations and different heat release rates. The results show that the flue gas reaching the working face varies greatly from different ignition source locations, and the smoke propagation time of the working face decreases first and then increases with the increase in the scale of the fire. The location of the fire source is from 0 to 700 m, and the visibility of the working face will drop to less than 3 m within 10 min, which seriously affects emergency evacuation; the maximum concentration of CO in the working face is proportional to the heat release rate, the fire source is less than 100 m away from the working face, and the temperature of the air inlet area of the working face is higher than 60 °C, which poses a great threat to personnel evacuation. When the fire source is less than 200 m away from the working face, the evacuees will encounter smoke damage on the working face, and when the fire scale reaches 4 MW and 6 MW, the CO concentration will have a great impact on the evacuation and make people incapacitated.

Keywords: mine fire; belt conveyor; smoke spread; numerical simulation; emergency evacuation



Citation: Wei, Y.; Li, A.; Li, Y.; Liang, W. Research on the Propagation Law of Fire Smoke on the Working Face of a Belt Conveyor. *Fire* **2024**, *7*, 405. <https://doi.org/10.3390/fire7110405>

Academic Editor: Haiyan Wang

Received: 8 October 2024

Revised: 26 October 2024

Accepted: 30 October 2024

Published: 5 November 2024



Copyright: © 2024 by the authors. Licensee MDPI, Basel, Switzerland. This article is an open access article distributed under the terms and conditions of the Creative Commons Attribution (CC BY) license (<https://creativecommons.org/licenses/by/4.0/>).

1. Introduction

The belt conveyor is the pivot of the coal transportation system in mines, and most coal mines currently use flame retardant tapes; however, due to its long conveying distance and long time of use, it is still easy for fire accidents to happen once it meets an ignition source or due to its own friction, etc. [1,2]. On 20 November 2015, a fire accident occurred in the tape lane of the Apricot Flower Coal Mine of the Jixi Mining Company of the Heilongjiang Long Coal Group, which resulted in 21 people being killed and 1 person being missing. At 0:20 on 27 September 2020, a major fire accident occurred in Songzao Coal Mine, Chongqing Nengtou Yu New Energy Co., Ltd. when coal was transported uphill by a No. 2 large-inclination belt conveyor under the well, resulting in 16 deaths and 42 injuries. On 24 September 2023, a fire accident occurred in a belt conveyor underneath the Shanzishu Coal Mine in Panzhou City, Guizhou Province, resulting in 16 deaths.

The main component of the tape is PVC, which produces not only CO and CO₂ but also HCL gas during the combustion process. In cases of fire, the smoke will spread to the roadways through the underground airflow, causing asphyxiation and poisoning of the workers [3]. The strong smoke will also reduce the visibility of the underground, which will adversely affect the evacuation of the personnel [4,5]. There have been many studies conducted by scholars in the area of mine fires. The CFD model was optimized by performing thermogravimetric analysis experiments and using the results for estimating gravimetric properties [6]. Through the simulation of branch tunnel fires in coal mines, it is found that branch tunnel fires have lower critical speeds, and a new calculation model is proposed [7]. Using the non-premixed PDF combustion model, the dynamic evolution law

of mine fires was studied, and the calculation model of the relationship between the length of the smoke return layer and the wind speed and inclination angle was established [8]. The effect of tunnel air velocity on the spread of mine fires was investigated, and it was found that the thickness and maximum temperature of the backflow layer decreased linearly with the increase in ventilation velocity [9]. Flame length correlation was assessed [10] alongside the amount of time necessary for people to escape [11,12]. A machine learning and neural network approach was utilized to predict the fire spread trend, providing a novel and effective method for rapid prediction of fire dynamics in mine tunnels [13–15]. Mine fires at different altitudes were simulated and experimented, and correlations were established to predict the longitudinal distribution characteristics of roof temperatures in mine fires at different altitudes [16]. Fire simulation was carried out using ANSYS for the roadway with different inclinations, and the spatial distribution of fire temperature was obtained [17]. Suppression of conveyor belt fires using sprinkler nozzle position, water flow rate, and activation temperature was studied by CFD modeling [18]. The safety of coal miners in the event of a fire can be maximized by establishing or improving fire emergency response systems [19].

From the above analysis, it can be seen that the purpose of the above study is mainly to conduct experimental and simulation studies on the specific parameters and general rules of mine tape fires. However, in addition to wind speed and fire source size, temperature, smoke distribution, CO concentration, visibility, etc. are important parameters to guide the evacuation of personnel when the fire source is located in different places and during different periods of fire development. Therefore, this paper takes the commonly used “U”-type ventilation comprehensive mining face as a simulation example and uses Pyrosim2019 fire simulation software to establish a model to simulate different fire source locations in the belt conveyor lane, different periods of fire, smoke concentration, visibility, CO concentration and temperature change in the face area, which are very important for guiding the preparation of emergency plans and the determination of disaster avoidance routes [20].

2. Fire Simulation Modeling

2.1. Geometric Model

The geometric model was 1.3 m/s, and the thickness of the wall of the roadway was 1 m; the initial temperature was 20 °C, and a series of ignition source points were set up at different locations of the belt conveyor road (transportation chute). The fire source area was taken as 2 m². A series of fire source points were set in different locations of the belt conveyor alley (i.e., the transportation chute), and the t_2 fire growth model was selected. PVC combustion produces a medium-velocity fire, and a fire growth coefficient of 0.01172 was assumed, as in a medium-speed fire growth model. The CO production rate of PVC combustion was set as 0.15 [21]. The fire size was uncertain; therefore, three heat release rate fires of 2 MW, 4 MW and 6 MW were set. In order to monitor various parameters in the tunnel after the fire, a series of smoke, visibility, CO, and temperature detectors were set up at a height of 1.8 m in the working face to simulate the distribution of smoke and CO in the tunnel after the fire. In modeling, the upwind direction of the transport downtrack was taken as the X-axis positive direction, the wind speed direction of the working face was taken as the Y-axis positive direction. The vertical direction was taken as the Z-axis direction. We set the farthest end of the belt conveyor alley (the X maximum position) as the main gate, and the farthest end of the return-airway as the tailgate; the fire model of the belt conveyor alley is shown in Figure 1. The spatial and temporal distribution of smoke and other fire hazard parameters in the working face were investigated by varying the location of the fire source and the rate of heat release. Therefore, we set up one fire source point at every distance in the belt conveyor roadway and distributed it in each location of the roadway to simulate the distribution of smoke, visibility, CO and temperature in the roadway of the working face after the occurrence of different sizes of fires.

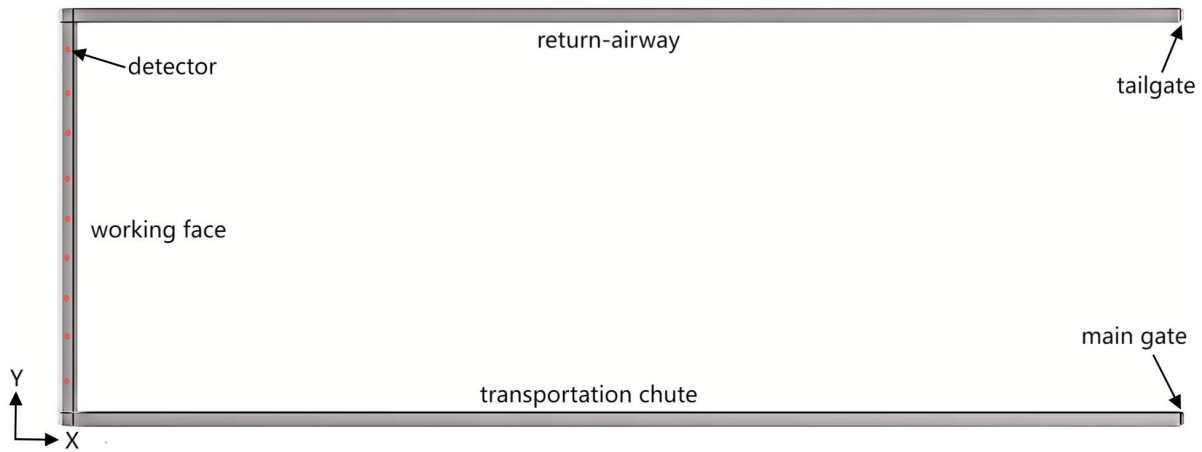


Figure 1. Schematic diagram of fire simulation in belt conveyor lane.

2.2. Meshing

FDS uses the grid as the smallest computational unit, and its size determines the spatiotemporal accuracy of the equations. It is divided into large grids, which reduces the number of grids and increases the simulation speed, but the results obtained are also rough. However, if the grid is too small, it will greatly increase the time taken for numerical computation. The characteristic diameter of the fire source can be calculated by the following equation [6]:

$$D^* = \left[\frac{Q}{\rho_{\infty} c_p T_{\infty} \sqrt{g}} \right]^{\frac{2}{5}} \tag{1}$$

Among them, Q , c_p , ρ_{∞} , and T_{∞} , respectively, are the heat release rate, air-specific heat capacity, air density, and ambient temperature.

The optimal values of $D^*\delta$ range from 4 to 16, and these values can be solved for all plume dynamics models and other geometrical properties. We simulate the fire temperature in the roadway with a fire power of 4 MW and compared the distribution of temperature at 100 m downstream of the fire source with different grid sizes of 0.5, 0.4, 0.3, and 0.2 m, as shown in Figure 2. The results show that the simulated temperature difference using different grid sizes was not very large, and the grid size was reduced from 0.3 m to 0.2 m. Therefore, in order to balance expected accuracy, time cost, and computer resources, in this study, the grid size was set to 0.3 m. Therefore, in order to be realistic and facilitate the computation, the grid size selected in this paper is 0.3 m × 0.3 m × 0.3 m for FDS simulations.

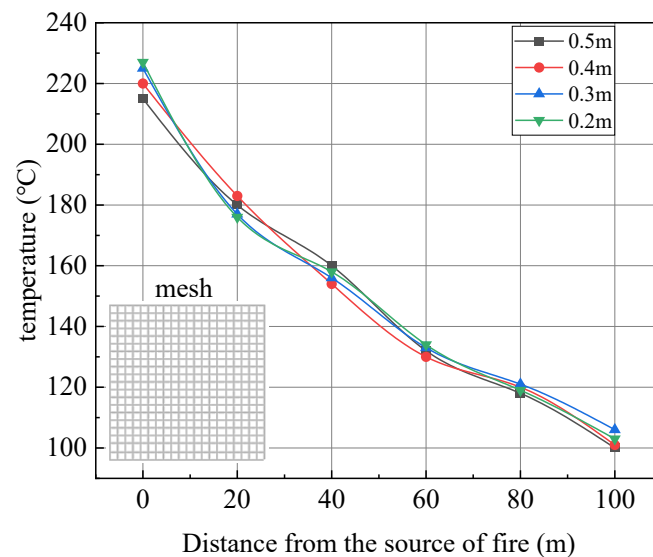


Figure 2. Temperature distribution of different grid sizes.

2.3. Physical Modeling of Alleyway Fires

The simulation software chosen for the FDS technique in this paper is Pyrosim, and the fire model chosen is a field model. It is a more complex turbulence mechanics model. The simulation methods used are the straight number numerical simulation method and the large eddy numerical simulation method, and the physical theory is based on the mass conservation equation, the material conservation equation, the energy conservation equation, and the momentum conservation equation.

The mass conservation equation is as follows:

$$\nabla \cdot (\rho u) + \frac{\partial \rho}{\partial t} = 0 \quad (2)$$

where u , ρ , and t , respectively, are the flow rate of the gas, the density of gas generated by combustion, and burning time.

The material conservation equation is as follows:

$$\frac{\partial}{\partial t}(\rho Y_i) + \nabla \cdot \rho Y_i u = \nabla \cdot \rho D_i \nabla Y_i + \bar{m} \quad (3)$$

where Y_i , D_i , and \bar{m} , respectively, are the Group i gas mass fraction, Group i gas diffusion coefficient, and Group i gas volume generation rate.

The energy conservation equation is as follows:

$$\frac{\partial}{\partial t}(\rho h) + \nabla \cdot \rho h u - \frac{\partial \rho}{\partial t} = q - \nabla \cdot q_r + \nabla \cdot \sum_i h_i (\rho D)_i \nabla Y_i \quad (4)$$

where h , q , q_r , and D , respectively, are the enthalpy, heat release rate, radiant heat flux, and gas diffusion coefficient.

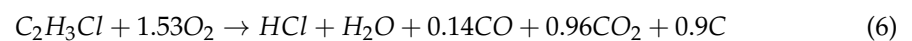
The momentum conservation equation is as follows:

$$\rho \frac{\partial u}{\partial t} + (u \cdot \nabla) u \rho + \nabla p = \rho g + f + \nabla \cdot \tau \quad (5)$$

where p , f , and τ are the barometric pressure value, external force value, and viscous force, respectively.

2.4. Single-Step Turnkey Reaction Model

PVC is a macromolecular substance with a molecular mass of usually more than 10,000. Therefore, the PVC molecular formula needs to be simplified to C_2H_3Cl . The reaction process is



2.5. Large Eddy Simulation (LES)

LESs are used to simulate the propagation and distribution of high-temperature toxic fumes on the working face during a belt conveyor fire. LES decomposes the turbulent motion into large-scale eddies and small-scale eddies, directly simulates the motion of large-scale eddies, and simulates the impact of small-scale eddies through the model. This method captures the transient characteristics of turbulence and the phenomenon of unsteady flow, which is very helpful for simulating the dynamic propagation and distribution of smoke during belt conveyor fires. It can provide detailed information on the flow of smoke at different times, such as the vortex structure of smoke and the change in diffusion velocity, which is of great significance for in-depth study of the propagation mechanism of smoke and the determination of dangerous areas.

2.6. K-Epsilon (k-ε) Model

When simulating the spread and distribution of high-temperature toxic fumes on the working surface during a belt conveyor fire, the k-epsilon (k-ε) model was selected as the turbulence model in the simulation. First of all, the calculation efficiency of this model is relatively high, and it has good practicality for actual engineering problems. Secondly, for the more complex scenario of a belt conveyor fire, the diffusion and turbulence characteristics of smoke can be simulated to a certain extent. The calculation formula of the standard k-ε model is as follows:

$$\frac{\partial(\rho k)}{\partial t} + \frac{\partial(\rho k u_i)}{\partial x_i} = \frac{\partial}{\partial x_i} \left[\left(\mu + \frac{\mu_t}{\sigma_k} \right) \frac{\partial k}{\partial x_j} \right] + G_k - \rho \epsilon \tag{7}$$

where $u_i, x, \mu, \mu_t, \sigma_k, G_k, \epsilon$, are the velocity components, coordinate components, molecular viscosity coefficient, turbulent viscosity coefficient, turbulent Trump number of turbulent kinetic energy k, turbulent kinetic energy generation term due to average velocity gradient, and dissipation rate, respectively.

$$\frac{\partial(\rho \epsilon)}{\partial t} + \frac{\partial(\rho \epsilon u_i)}{\partial x_i} = \frac{\partial}{\partial x_i} \left[\left(\mu + \frac{\mu_t}{\sigma_\epsilon} \right) \frac{\partial \epsilon}{\partial x_j} \right] + C_{1\epsilon} \frac{\epsilon}{k} G_k - C_{2\epsilon} \rho \frac{\epsilon^2}{k} \tag{8}$$

where $\sigma_\epsilon, C_{1\epsilon}$ and $C_{2\epsilon}$ are the turbulent Trump numbers of the dissipation rate ϵ and are empirical constants.

2.7. Analysis of Fire Risk Factors of Belt Conveyor
Analysis of Fire Smoke Spreading Pattern

The temperature of fire smoke is high, and when it spreads, it will first rise to the top and then spread downward and to the ends [22]. We placed a fire source every 200 m from 0 to 2000 m, both in the upper corner of the working face and the lower corner of the smoke detector at 1.8 m, in order to simulate a fire of 4 MW and a corresponding smoke flow and time, the results of which are shown in Table 1. As shown, when the location of the fire source was greater than or equal to 800 m, the smoke took longer than 600 s to pass through the working face. The workers would in this case have enough time to leave the working face because the smoke would need a longer time to pose a threat to the workers at the working surface. Therefore, emphasis should be placed on the study of the spread of smoke across the working face from fire sources located from 0 to 700 m, which would take less than 10 min to cause a threat. Table 2 shows the time required for smoke to cross the 180 m working face for different fire conditions. When the distance between the fire source and the working face is 0 m, the longest time is required for the smoke to spread to the whole working face (1.8 m height), and the time required for the smoke to spread decreases and then increases with the increase in the location of the fire source. The fire source locations corresponding to the lowest smoke spread times for fire sizes of 2 MW, 4 MW, and 6 MW were 100 m, 200 m, and 300 m.

Table 1. Flue gas flow time at different ignition source locations.

Location of fire source/m	0	200	400	600	800	1000	1200	1400	1600	1800	2000
Bottom corner angle/s	5	105	208	305	488	621	761	904	1047	1189	1333
Top Corner Angle/s	144	194	303	412	608	734	871	1024	1164	1306	1450

Table 2. The time for flue gas to pass through the working face under different working conditions.

—	Location of Fire Source/m	0	100	200	300	400	500	600	700
Size of the fire	2 MW	131 s	92 s	98 s	104 s	108 s	113 s	116 s	120 s
	4 MW	139 s	98 s	89 s	93 s	95 s	102 s	107 s	115 s
	6 MW	144 s	104 s	93 s	91 s	93 s	100 s	109 s	113 s

Figures 3–5 show the flue gas concentration at a height of 1.8 m at the working face after 600 s under different working conditions, and the horizontal axis is the position coordinates of the working face. The data in the figure show that the concentration of smoke near the fire source is very low, and the concentration of smoke at 600 m and 700 m from the fire source varies greatly at different locations of the working face, because the fire source is too far away from the working face. The larger the heat release rate, the higher the smoke concentration, and the maximum smoke concentration reached more than 90% when the fire scale was 6 MW.

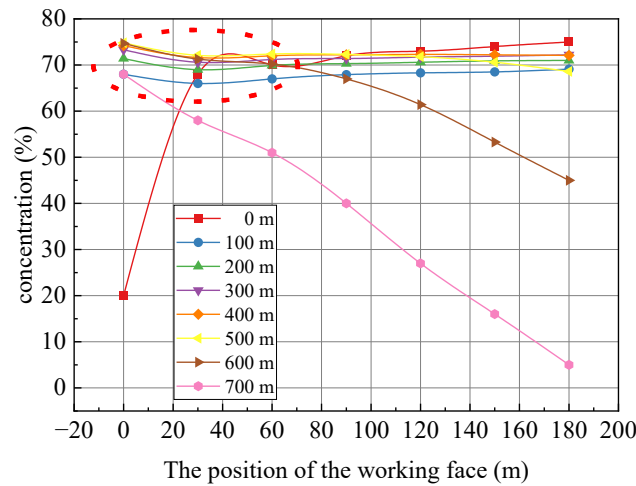


Figure 3. The maximum concentration of smoke at the 2 MW working face with fire scale.

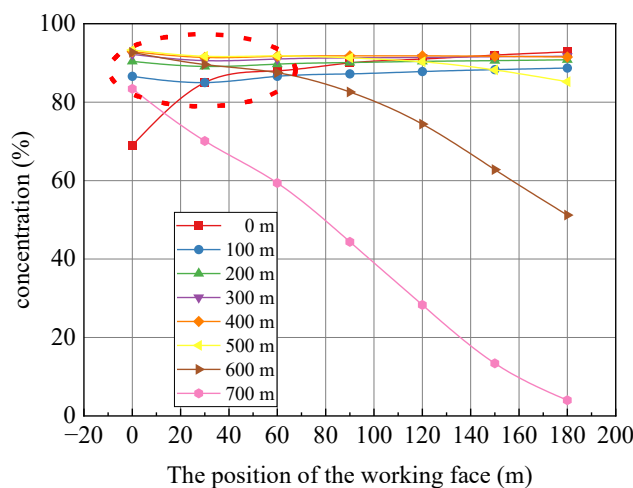


Figure 4. The maximum concentration of smoke at the 4 MW working face with fire scale.

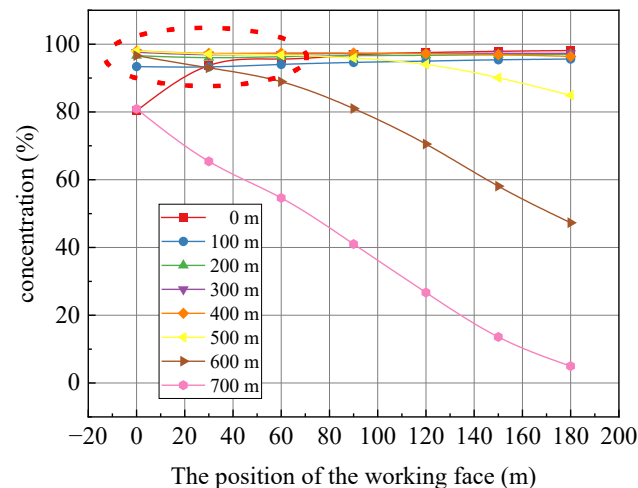


Figure 5. The maximum concentration of smoke at the 6 MW working face with fire scale.

From Figures 3–5, it can be seen that the concentration of smoke arriving at the working face showed a decreasing tendency 30 m before the working face (dotted line in the figure), and it tended to stabilize after 30 m. When the smoke flowed through the corner, the velocity decreased due to local resistance. When the flue gas flowed through the corner, due to local resistance, the speed decreased, the flue gas started to gather, the concentration increased, the excess flue gas caused the air pressure to rise, and a difference in pressure formed with the roadway of the working face, which accelerated the flow of flue gas again. Thus, as we see in the figure, the concentration of the flue gas decreased at 30 m in front of the working face. The concentration of flue gas in front of the working face decreased after the flue gas reached the 2 MW heat exchanger. This law was most obvious with a heat release rate of 2 MW; the heat release rate increased as the concentration difference decreased, and this phenomenon was less significant with a heat release rate of 6 MW, when the concentration of flue gas was very high everywhere across the working face.

2.8. Fire Visibility Analysis

Fire smoke is not only toxic and harmful; the solid particles in it also reduce visibility and affect the escape speed of personnel. According to the walking speed and visibility function of KARL [23], visibility below 3 m has an effect on the walking speed of personnel. Figures 6–8 demonstrate the time required for visibility to drop to 3 m for different fire distances at a height of 1.8 m on the working face. The data show that at the same position on the working face, the time for visibility to fall to 3 m increases by about 70 s with an increase of 100 m in the position of the fire source; at the same position of the fire source, the distance from the working face and the time required for visibility to fall to 3 m are in a one-time function relationship. For the working personnel at the working face, when the fire source is close to the working face, the smoke will spread into the working face in a short time, resulting in a rapid decrease in visibility, which seriously affects the evacuation of personnel; at this time, the time for emergency evacuation is only about 200 s.

When the distance of the fire source X is 700 m, the visibility of the working face from 90 to 180 m is more than 3 m within 10 min after the fire occurs, indicating that the visibility within 10 min has no great impact on the operators in the second half of the working face. Moreover, it is not that the larger the scale of the fire, the wider the range of visibility of less than 3 m. The data in the figure show that under the condition of $X = 700$ m, when the fire scale is 2 MW and 6 MW, the visibility range of less than 3 m only reaches the position of 80 m of the working face. When the fire scale is 4 MW, this range is increased to 90 m of the working face.

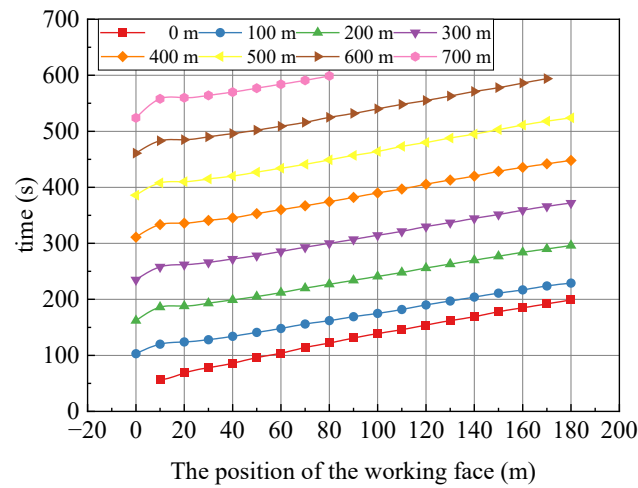


Figure 6. The time when the visibility of the 2 MW working face drops to 3 m in the scale of the fire.

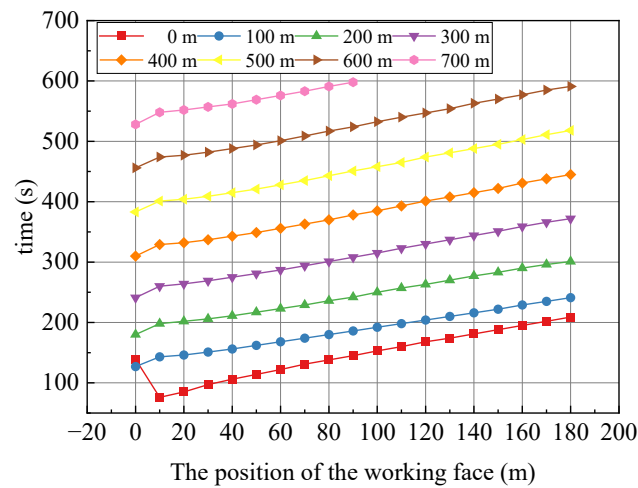


Figure 7. The time when the visibility of the 4 MW working face drops to 3 m in the scale of the fire.

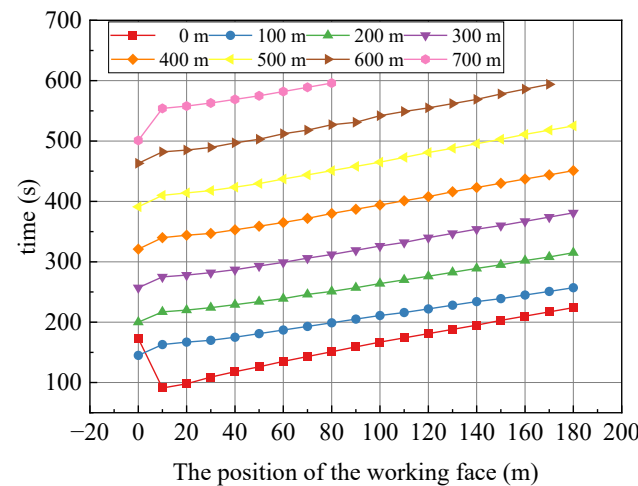


Figure 8. The time when the visibility of the 6 MW working face drops to 3 m in the scale of the fire.

2.9. Fire CO Analysis

As a harmful gas that can cause great harm to human beings, many scholars have analyzed and predicted the concentration of CO in fires [24–26]. Coal Mine Safety Regulations stipulate that the allowable concentration of CO for underground operations is 24 ppm. When the air content is 1×10^3 ppm, people who are stranded in this environment will

experience headaches and nausea; when the content reaches 5×10^3 ppm, a person will die within 20–30 min; and at 1×10^4 ppm, death occurs within 1–2 min.

The maximum CO concentration at the working face within 10 min with different fire scales and different ignition source locations was obtained, as shown in Figures 9–11. If the ignition source is close to the working face, the CO concentration in the working face should be stable and not increase. When the location of the ignition source is less than or equal to 400 m, the CO concentration reaches stability, and when the ignition source location is 100 m, 200 m, 300 m, and 400 m, the maximum CO concentration is relatively close considering the same fire scale. The maximum CO concentration is proportional to the fire scale in the area in which the CO concentration is relatively stable. The CO concentrations in the working face are all well above the normal value, which is dangerous for the trapped people. At a distance of 700 m from the working face, the CO concentration is mostly more than 200 ppm, and when the fire scale is 2 MW, the maximum value of CO stability is below 800 ppm and above 500 ppm. When the fire scale is 4 MW, the maximum value of CO stability is below 1600 ppm and above 1000 ppm. When the fire scale is 6 MW, the maximum value of CO stability is below 2400 ppm and above 1500 ppm. Although these concentrations of CO will not cause death in the short term, they will cause uncomfortable symptoms such as nausea and dizziness among the trapped people, affect the escape speed, and may even cause fainting due to poisoning in severe cases.

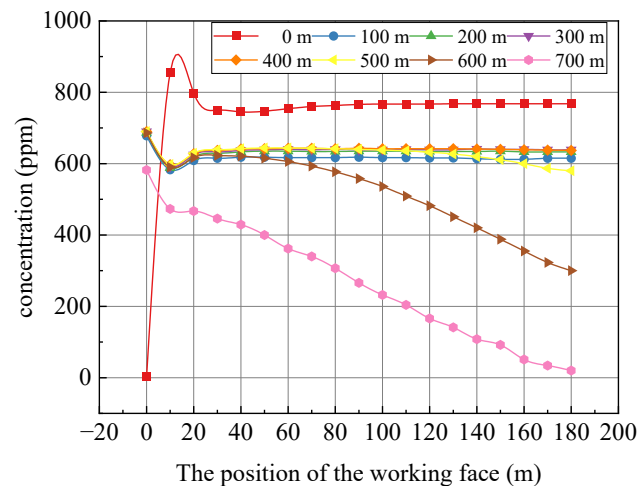


Figure 9. The maximum concentration of CO in the 2 MW fire at the working face.

When a fire occurs, the temperature near the fire source can quickly reach several hundred degrees Celsius, damaging the human respiratory tract and causing a rapid drop in blood pressure and respiratory failure; at the same time, the blood vessels may become congested and cause pulmonary edema [27]. When the temperature reaches 55°C , the skin will blister due to burns. At 60°C , people can normally survive for a period of time, but the body will eventually experience a coma-like phenomenon; if not treated in time, the body may go into shock.

Figures 12–14 show the maximum temperature at each location of 1.8 m at the working face for different fire sizes and different fire source locations within 10 min. Due to the influence of temperature stratification and wall heat transfer, with the three fire sizes, the temperature at the working face does not exceed 50°C when the fire source distance is more than 300 m, which is safer for the personnel. When the fire source location is 200 m, the temperature in some locations of the working face with 4 MW and 6 MW fires exceeds 50°C but does not reach 60°C , so any trapped personnel will suffer burns after being exposed for a certain period of time. When the fire source is 100 m away from the working face, the maximum temperature at 0 m of the working face is close to 80°C , and the maximum temperature of the 4 MW and 6 MW fires at the working face exceeds 100°C . The overall temperature at the working face is high, so it is necessary to evacuate from the working face

as soon as possible so that lives are not endangered. When the fire source is 0 m away from the working face, the temperature of the working face with all three fire scales is much higher than the normal ambient temperature, and the temperature at 180 m from the working face exceeds 50 °C, which requires immediate evacuation of the working face.

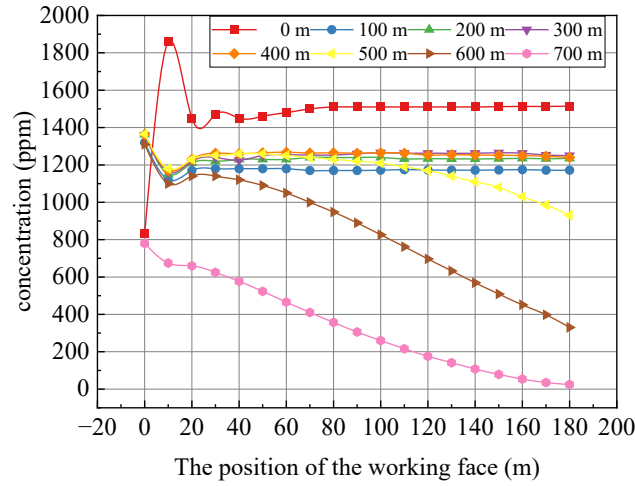


Figure 10. The maximum concentration of CO in the 4 MW fire at the working face.

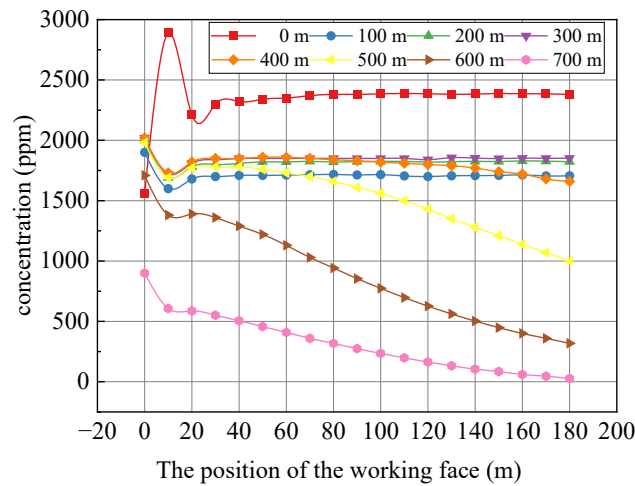


Figure 11. The maximum concentration of CO in the 6 MW working face of the fire scale.

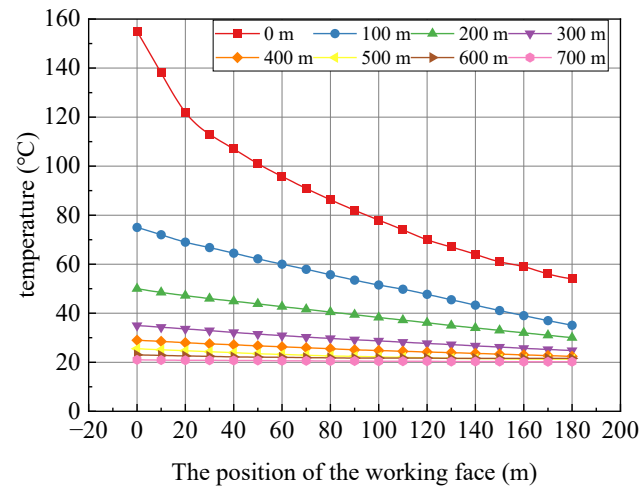


Figure 12. The maximum temperature of the working face with a fire scale of 2 MW.

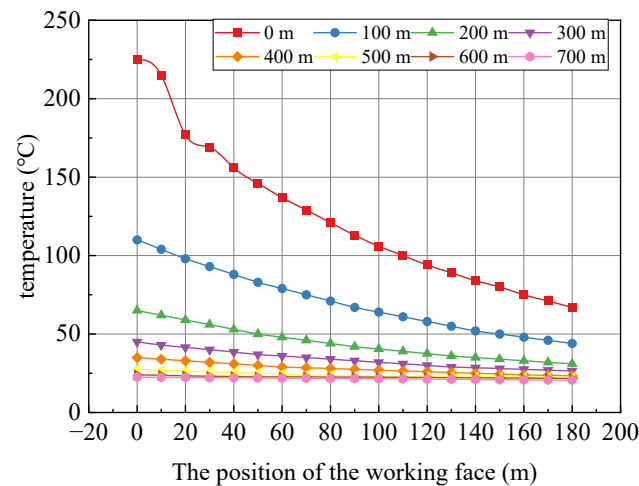


Figure 13. The maximum temperature of the working face with a fire scale of 4 MW.

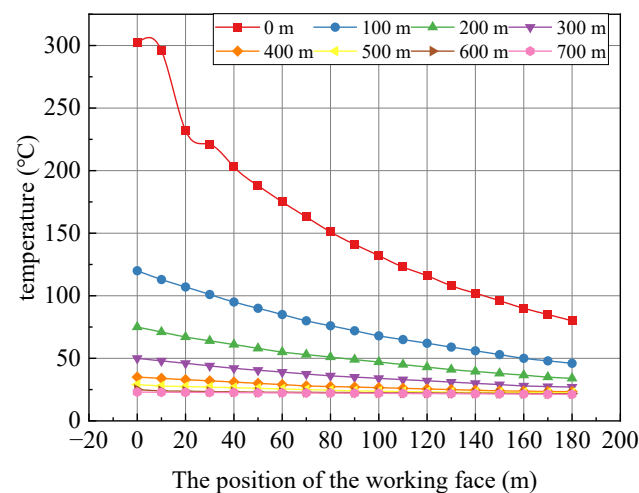


Figure 14. The maximum temperature of the working face with a fire scale of 6 MW. Analysis of fire emergency evacuation.

The distance and temperature in the graph become a curved relationship, with the distance increasing whilst the decrease in temperature is more gentle, in line with the law of exponential decay in temperature. Comparing the temperature at the working face at 100 m when the fire source is located at 0 m and the temperature of the working face at 0 m when the fire source is located at 100 m, it is found that these two temperatures are roughly equal, and these two locations are 100 m away from the flow of smoke. We then carried out similar comparisons in turn, and the temperatures were still roughly equal, which means that the corners of the roadway do not have a great influence on temperature attenuation.

When a fire breaks out, it is important for workers to be able to evacuate in a timely manner [28]. Under the mine, the environment is complex; it is inconvenient for personnel to walk through, and the actual evacuation speed of the site is roughly 1.5 m/s. It also takes a certain amount of time for the operator who discovers the fire to make a decision (around 60 s), and the operator across the face needs a maximum of 120 s. The length of the return-airway is 2200 m, and the evacuation time to reach the end of the return-airway is 1466 s, meaning the total evacuation time is 1646 s. According to Table 2, if the location of the fire source is greater than 200 m, the workers can safely evacuate to the return-air lane without being exposed to smoke. However, due to the long return-air lane of the working face, the time taken to walk through the return-air lane is more than 20 min, and speed decreases with physical exertion. It is therefore easy to encounter a high concentration of smoke when arriving in the return-air lane, which affects a normal escape. According to

the data, it can also be inferred that when the fire source is more than 1000 m away from the working face, the probability of safely crossing the return-air alley is very high. Because of the uncertainty of the location of the fire, the workers may encounter the smoke at the working face or at a certain location in the return-air alley; therefore, in the evacuation analysis, a most unfavorable situation is assumed, due to the malfunctioning of the fire alarms and improper on-site handling, which means workers escape to the return-air alley when the concentration of smoke in the alley has reached its maximum; we investigated the evacuation time of the workers at this time.

The factors affecting evacuation speed in a fire are visibility, CO concentration, and temperature, and scholars at home and abroad have derived a relational equation of the influence of each factor on evacuation speed in a fire based on experimental data [29]. The visibility influence coefficient is f_m , the CO influence coefficient is f_c , and the temperature influence coefficient is f_θ .

When the visibility is greater than 3 m, the visibility influence coefficient f_m is always 1. In this paper, after the fire develops to the stabilization stage, the visibility reached as low as 2.5 m, 1.15 m, and 0.8 m at heat release rates of 2 MW, 4 MW, and 6 MW, respectively.

A CO concentration of less than 0.1% has no effect on the evacuation rate, a CO concentration greater than 0.25% has an evacuation rate of 0, and fire-stranded workers will be incapacitated for a short period of time. The average CO concentration can reach 0.06%, 0.12%, 0.18% at heat release rates of 2 MW, 4 MW and 6 MW; the exposure time is not definite, and the workers will be incapacitated after exceeding a certain exposure time. The maximal exposure time is 20 min at a concentration of 0.12%, and the maximal exposure time is 11 min at a concentration of 0.18%. Workers will normally pass through the return-air alley after more than 20 min, and the workers will be incapacitated after evacuating a certain distance in the presence of these two concentrations of CO.

The fire temperature decreases exponentially with distance, and the return-air lane is far away from the fire source point; the temperature is generally not high, and the average temperature is lower than 30 °C. Thus, the effect of temperature on the workers can be ignored, and f_θ is taken 1.

The combined evacuation speed of personnel v is given in the following equation:

$$v = v_0 \times f_m \times f_c \times f_\theta \tag{9}$$

In the formula, v_0 is the maximum evacuation speed.

The evacuation factors considering heat release rates of 2 MW, 4 MW and 6 MW are shown in Table 3.

Table 3. Evacuation factors at different heat release rates.

	f_m	f_c	f_θ	v	ASET
2 MW	0.83	1	1	1.25 m/s	1760 s
4 MW	0.37	—	1	—	—
6 MW	0.25	—	1	—	—

As can be seen from Table 3, the evacuation time in the return-air alley was 1760 s at a heat release rate of 2 MW, which was 294 s or about 5 min more than the normal time, and at this time, the temperature and CO had basically no effect on human functioning. When the heat release rate reached 4 MW or more, the workers were exposed to a high concentration of CO for too long to evacuate to the end of the return-airway.

As the length of the working face roadway is more than 2000 m, the time required to cross the return-airway is too long. If the location of the fire source is farther away from the working face, the workers will have more time to evacuate, and there is a high probability that they cross the return-airway, but if the fire source is closer to the working face, it will

be difficult for the workers to be safely evacuated if they cannot save themselves in time or if they use counter-ventilating measures.

3. Conclusions

- (1) The time for the smoke to reach the working face varies greatly among different fire source locations, and it takes at least 10 min for the smoke to reach the working face after the fire source location exceeds 800 m. At the same time, the smoke spreading time decreases and then increases as the fire source distance increases. At the same time, as the distance from the fire source increases, the working face smoke spreading time first decreases and then increases; when the smoke concentration is greater than 70%, there will be a gathering phenomenon in the corners of the roadway, at which point the concentration in the corners is higher than the concentration of the two sides. The concentration then reaches more than 90%, showing basically no difference.
- (2) The data illustrate that the visibility of the workplace at fire source locations less than 500 m all dropped below 3 m within 10 min after the fire, seriously affecting evacuation. At the same fire size, the maximum CO concentrations were all relatively close to each other, at 600 ppm, 1200 ppm, and 1800 ppm, respectively, and the maximum CO concentration in the workplace was proportional to the fire size. Within 10 min of the fire, the temperature of the working face did not cause much harm in the short term when the fire's point of origin was 300 m away from the working face.
- (3) After a fire, the theoretical normal evacuation time of the workers exceeds 20 min, and workers will encounter smoke at the working face when a fire occurs within 200 m of the working face. According to our analysis of the most unfavorable principles of fire, the temperature does not affect the evacuation speed of the return-air lane, but visibility has a great influence on evacuation, and the influence coefficient of the visibility is minimized to 0.25. When the fire size is 2 MW, the concentration of CO in the smoke has no influence on the evacuation speed, but when the fire size reaches 4 MW and 6 MW, the concentration of CO has a great influence on evacuation and can incapacitate people.

Author Contributions: Conceptualization, Y.W. and A.L.; methodology, Y.W. and A.L.; software, A.L.; validation, A.L. and Y.L.; investigation, W.L.; data curation, W.L.; writing—original draft preparation, Y.W., A.L., Y.L. and W.L.; writing—review and editing, A.L.; supervision, Y.W.; All authors have read and agreed to the published version of the manuscript.

Funding: This research received no external funding.

Conflicts of Interest: The authors declare no conflict of interest.

References

1. Barros-Daza, M.J.; Luxbacher, K.D.; Lattimer, B.Y.; Hodges, J.L. Mine conveyor belt fire classification. *J. Fire Sci.* **2022**, *40*, 44–69. [[CrossRef](#)]
2. Shi, D.; Liu, X.; He, L. A Review on Mine Fire Prevention Technology and Theory Based on Bibliometric Analysis. *Sustainability* **2023**, *15*, 16639. [[CrossRef](#)]
3. Aksoy, C.O.; Aksoy, G.G.U.; Fisne, A.; Alagoz, I.; Kaya, E. Investigation of a conveyor belt fire in an underground coal mine: Experimental studies and CFD analysis. *J. S. Afr. Inst. Min. Metall.* **2023**, *123*, 589–597. [[CrossRef](#)]
4. Guo, R.; Ma, L.; Fan, J.; Wang, W.; Wei, G.; Ren, L. Temperature Distribution of Coal Mine Tunnel Fire During Dynamic Sealing Process: A Numerical Study. *Combust. Sci. Technol.* **2024**, *196*, 55–72. [[CrossRef](#)]
5. Wang, W.; Liu, H.; Yang, B.; Zhang, D.; Lyu, H.; Song, X.; Shu, C.-M. Pyrolysis characteristics and dynamics analysis of a coal mine roadway conveyor belt. *J. Therm. Anal. Calorim.* **2023**, *148*, 4823–4832. [[CrossRef](#)]
6. Yuan, L.; Mainiero, R.J.; Rowland, J.H.; Thomas, R.A.; Smith, A.C. Numerical and experimental study on flame spread over conveyor belts in a large-scale tunnel. *J. Loss Prev. Process Ind.* **2014**, *30*, 55–62. [[CrossRef](#)]
7. Zhu, H.; Qu, B.; Wang, J.; Hu, L.; Yao, Y.; Liao, Q. Numerical study on the smoke movement and control in main roadway for mine fires occurred in branch. *Case Stud. Therm. Eng.* **2023**, *45*, 102938. [[CrossRef](#)]
8. Wen, H.; Liu, Y.; Jin, Y.; Zhang, D.; Guo, J.; Li, R.; Zheng, X. Numerical Simulation for Mine Oblique Lane Fire Based on PDF Non-Premixed Combustion. *Combust. Sci. Technol.* **2021**, *193*, 90–109. [[CrossRef](#)]

9. Li, L.; Si, J.; Li, Z. Characteristics of the spatial and temporal evolution of the environmental parameters for belt fire in underground coal mine roadway. *Case Stud. Therm. Eng.* **2023**, *49*, 103346. [[CrossRef](#)]
10. Hansen, R. Fire behaviour of multiple fires in a mine drift with longitudinal ventilation. *Int. J. Min. Sci. Technol.* **2019**, *29*, 245–254. [[CrossRef](#)]
11. An, W.; Li, Q.; Liang, K.; Yin, X.; Wang, Z. Study on Combustion Characteristics and Evacuation during Intake Airway Fire in Coal Face under Different Ventilation Conditions. *Combust. Sci. Technol.* **2021**, *193*, 1378–1399. [[CrossRef](#)]
12. Niu, H.-Y.; Qiao, C.-L.; An, J.-Y.; Deng, J. Experimental study and numerical simulation of spread law for fire on tunnel. *J. Cent. South Univ.* **2015**, *22*, 701–706. [[CrossRef](#)]
13. Barros-Daza, M.J.; Luxbacher, K.D.; Lattimer, B.Y.; Hodges, J.L. Real Time Mine Fire Classification to Support Firefighter Decision Making. *Fire Technol.* **2022**, *58*, 1545–1578. [[CrossRef](#)]
14. Chen, Y.; Liu, J.; Zhou, Q.; Liu, L.; Wang, D. A study on rapid simulation of mine roadway fires for emergency decision-making. *Sci. Rep.* **2024**, *14*, 1674. [[CrossRef](#)]
15. Hong, Y.; Kang, J.; Fu, C. Rapid prediction of mine tunnel fire smoke movement with machine learning and supercomputing techniques. *Fire Saf. J.* **2022**, *127*, 103492. [[CrossRef](#)]
16. Wu, E.; Huang, R.; Wu, L.; Shen, X.; Li, Z. Numerical Study on the Influence of Altitude on Roof Temperature in Mine Fires. *IEEE Access* **2020**, *8*, 102855–102866. [[CrossRef](#)]
17. Liu, Y.; Duan, Z.; Cui, Y.; Jiang, F.; Gao, F.; Cui, M.; Tian, Z. Study on Smoke Temperature Distribution Characteristics of Coal Mine Inclined Roadway Fire. *Combust. Sci. Technol.* **2023**, *195*, 1–22. [[CrossRef](#)]
18. Yuan, L.; Smith, A.C. Numerical modeling of water spray suppression of conveyor belt fires in a large-scale tunnel. *Process Saf. Environ. Prot.* **2015**, *95*, 93–101. [[CrossRef](#)]
19. Wang, K.; Jiang, S.; Ma, X.; Wu, Z.; Shao, H.; Zhang, W.; Cui, C. Numerical simulation and application study on a remote emergency rescue system during a belt fire in coal mines. *Nat. Hazards* **2016**, *84*, 1463–1485. [[CrossRef](#)]
20. Wen, H.; Liu, Y.; Guo, J.; Zhang, Z.; Liu, M.; Cai, G. Study on Numerical Simulation of Fire Danger Area Division in Mine Roadway. *Math. Probl. Eng.* **2021**, *2021*, 6646632. [[CrossRef](#)]
21. Wang, W. Pyrolysis and Combustion Characteristics of Coal Mine Conveyor Belt. Ph.D. Thesis, China Coal Research Institute, Beijing, China, 2023.
22. Zhang, X. Underground Mine Fire Simulation Using Multiscale Modeling Approach. Ph.D. Thesis, Missouri University of Science and Technology, Rolla, MO, USA, 2012.
23. Fridolf, K.; Nilsson, D.; Frantzich, H.; Ronchi, E.; Arias, S. Walking speed in smoke: representation in life safety verifications. In Proceedings of the 12th International Conference on Performance Based Codes and Fire Safety Design Methods, Oahu, HI, USA, 23–27 April 2018.
24. Kursunoglu, N.; Ankara, H. Application of Statistical Process Control to Monitor Underground Coal Mine Fires Based on CO Emissions. *Combust. Sci. Technol.* **2024**, *196*, 142–159. [[CrossRef](#)]
25. Yuan, L.; Zhou, L.; Smith, A.C. Modeling carbon monoxide spread in underground mine fires. *Appl. Therm. Eng.* **2016**, *100*, 1319–1326. [[CrossRef](#)] [[PubMed](#)]
26. Zhou, L.; Yuan, L.; Bahrami, D.; Thomas, R.A.; Rowland, J.H. Numerical and experimental investigation of carbon monoxide spread in underground mine fires. *J. Fire Sci.* **2018**, *36*, 406–418. [[CrossRef](#)] [[PubMed](#)]
27. Yi, X.; Lei, C.; Deng, J.; Ma, L.; Fan, J.; Liu, Y.; Bai, L.; Shu, C.-M. Numerical Simulation of Fire Smoke Spread in a Super High-Rise Building for Different Fire Scenarios. *Adv. Civ. Eng.* **2019**, *2019*, 1659325. [[CrossRef](#)]
28. Salami, O.B.; Xu, G.; Kumar, A.R.; Pushparaj, R.I. Underground mining fire hazards and the optimization of emergency evacuation strategies (EES): The issues, existing methodology and limitations, and way forward. *Process Saf. Environ. Prot.* **2023**, *177*, 617–634. [[CrossRef](#)]
29. Zhu, S. Research on Composite Simulation of Evacuation of Construction Personnel Based on Fire Dual-Zone Model. Master's Thesis, Central South University, Changsha, China, 2010.

Disclaimer/Publisher's Note: The statements, opinions and data contained in all publications are solely those of the individual author(s) and contributor(s) and not of MDPI and/or the editor(s). MDPI and/or the editor(s) disclaim responsibility for any injury to people or property resulting from any ideas, methods, instructions or products referred to in the content.